Extragalactic large-scale structures in the northern Zone of Avoidance

M Ramatsoku[1], R C Kraan-Korteweg[1], A C Schröder[2] and W van Driel[3]

[1]Astrophysics, Cosmology and Gravity Centre (ACGC), Department of Astronomy, University of Cape Town, Private Bag X3, Rondebosch 7701, South Africa.
[2]South African Astronomical Observatory (SAAO), PO Box 9, 7935 Observatory, Cape Town, South Africa.
[3]GEPI, Observatoire de Paris, CNRS, Universit Paris Diderot, 5 place Jules Janssen, 92190 Meudon, France.

E-mail: mpati.ramatsoku@ast.uct.ac.za, kraan@ast.uct.ac.za, anja@hartrao.ac.za, wim.vandriel@obspm.fr

Abstract. We used the Nançay Radio Telescope to measure the 21 cm line emission of near-infrared bright galaxies in the northern Zone of Avoidance (ZoA) without previous redshift determinations. We selected galaxies with extinction-corrected magnitudes $K_s^o \leq 11\overset{\mathrm{m}}{.}25$ from the 2MASS Extended Source Catalog. These data will complement the existing 2MASS Redshift Survey (2MRS; first data release) as well as the ongoing 2MASS Tully-Fisher survey, both of which exclude the inner ZoA ($|b| < 5^\circ$), where the identification of galaxy candidates is the hardest. Of the ∼1000 identified 2MASX galaxy candidates we have so far detected 252 to our 3 mJy rms sensitivity limit and the velocity limit of 10500 km s^{-1}. The resulting redshift distribution reveals various new structures that were hitherto uncharted. They seem to form part of the larger Perseus-Pisces Supercluster. The most conspicuous is a ridge at about $\ell \approx 160^\circ$,$v \approx 6500$ km s^{-1}. Within this wall-like structure, two strong radio galaxies (3C 129 and 3C 129.1) are embedded which lie at the same distance as the ridge. They seem to form part of an X-ray cluster. Another prominent filament has been identified crossing the ZoA at $\ell \approx 90^\circ$, hence suggesting the second Perseus-Pisces arm is more extended than previously thought.

1. Introduction

Dust extinction and high stellar densities in the Galactic Plane block a large fraction of the sky resulting in the so-called Zone of Avoidance (ZoA) [1]. Compared to the optical, the near-infrared (NIR) is much less affected by the dust obscuration. A whole-sky near-infrared (JHK) imaging survey exists in the form of the 2-Micron All Sky Survey (2MASS)[2]. The resulting extended source catalogue, 2MASX, with its 1.6 million sources complete to $K_s \leq 13\overset{\mathrm{m}}{.}5$ [3], provides the most uniform and deep NIR sample of the whole sky. Although 2MASX suffers little from dust extinction, there remains an "NIR ZoA" caused by stellar crowding around the Galactic bulge ($\ell \lesssim \pm\, 90^\circ$) [1].

To analyse the large-scale galaxy distribution over the entire sky, the optical 2MASS Redshift Survey (2MRS) was started about a decade ago. The first data release is complete to $K_s^o = 11\overset{\mathrm{m}}{.}25$ [4], the second to $K_s^o = 11\overset{\mathrm{m}}{.}75$ [5]. Both versions do exclude, however, the inner ZoA ($|b| \leq 5^\circ$)

because of the inherent difficulties in getting good signal-to-noise (SNR) optical spectra for these heavily obscured galaxies. While the 2MRS is currently the deepest "whole-sky" redshift survey for mapping large-scale structures, and studying the dynamics in the nearby Universe and the CMB dipole [6], the lack of redshift data in the ZoA remains an obstacle. This also holds for the 2MASS Tully Fisher survey (2MTF) which uses a subsample of sufficiently inclined 2MASX spiral galaxies to study cosmic flow fields [7].

To improve on this we have started a project to systematically observe in H I all likely 2MASX galaxies in the "2MRS ZoA" without previous redshift information. The line emission from neutral hydrogen (H I) at the radio wavelength of 21 cm can travel unhindered through the thickest dust layers of the Milky Way. Targeting ZoA galaxies with a radio telescope will therefore allow us to obtain redshifts for gas-rich 2MASS galaxies. We used the 100m-class Nançay Radio Telescope (NRT) for pointed observations of all ZoA galaxies with Dec $> -39°$. We were particularly interested in filling in the northern ZoA because – contrary to the southern ZoA – most of the northern ZoA has not been surveyed in any systematic way before. For the southern hemisphere a blind H I survey has been performed with the Parkes Multi-Beam receiver (HIZOA) which covers $|b| < 5°$ for the longitude range $196° \leq \ell \leq 52°$ out to velocities of 12700 km s^{-1} (rms $\approx$ 6mJy)[8], [9]. For the remaining ZoA ($196° \gtrsim \ell \gtrsim 52°$) hardly any data is available (see e.g. the top panel of Fig.1).

2. Filling in the redshift gap in the ZoA

2.1. Sample selection

To start filling in the northern redshift gap we first extracted all extended sources from 2MASX with $|b| \leq 10°$ and extinction-corrected magnitudes $K_s^o \leq 11\overset{\mathrm{m}}{.}25$, i.e., the completeness limit of the first 2MRS catalogue and the 2MTF. Of the 4743 extended sources accessible to the Nançay Radio Telescope (Dec $> -39°$), we classified 2546 sources as clear galaxies (plus 42 as possible galaxies) by visually inspecting the Digitized Sky Survey (DSS)[1] images in the B_J, R and I bands, the 2MASS J and K-bands, as well as the 2MASX colour images. From that sample we excluded galaxies that already had redshift measurements by cross-correlating our catalogue with NED and unpublished data sets like 2MRS (Macri, priv comm), HIZOA (Kraan-Korteweg et al, priv comm), etc.

The final NRT target sample consists of ∼1000 near-infrared bright galaxy candidates in the ZoA ($-20° \lesssim \ell \lesssim 270°$; $|b| \leq 10°$); the great majority ($\gtrsim 83\%$) of them are located in the $|b| < 5°$ strip. We have already used 1200 hours of observing time with the NRT for pointed observations of these objects since mid-2009.

2.2. Observations and data reduction

The galaxy candidates were observed with the Nançay Radio Telescope in position-switching mode. Pairs of equal-duration ON/OFF-source integrations were made, with the OFF-source position $20'$ east of the target. Candidates were typically observed for 40-minute long periods till an rms noise level of 3 mJy was reached. Because none of the target galaxies have prior redshift information, the auto-correlator was set to cover a radial velocity range of -500 to 10500 km s^{-1}. The original resolution is 2.6 km s^{-1}, which is later smoothed to 18 km s^{-1} for further analysis. Observations were made simultaneously in two linear polarizations, to gain sensitivity. Data reduction and RFI recognition and mitigation were performed using the NAPS and SIR data reduction packages, developed by the NRT staff.

[1] http://stdatu.stsci.edu/dss/

2.3. Results

From July 2009 to March 2012, we observed 926 out of the total of 1000 target galaxies to an rms level of 3.0 mJy. The resulting spectra were first inspected by eye by one of us for the signature of redshifted galactic H I-emission. The reliability of all potential H I detections was then assessed independently by three other team members, followed by an adjudication by another team member. Clear detections, and non-detections which had reached our target rms noise level of 3 mJy were filed as such, whereas marginal or possible detections were tagged for re-observation, whose results were continuously updated.

This has led to 252 solid detections so far out of the 926 observed targets, i.e., a detection rate of 27%. This is a respectable detection rate given that no pre-selection was made according to morphological type (which is not straightforward in the NIR, nor in the ZoA). The mean rms in the final spectra was found to be 2.9 mJy. The 252 detected H I profiles have peak signal-to-noise ratios of $\gtrsim 5.0$.

A reliable detection was found to have a typical linewidth- and flux-dependent $\mathrm{SNR}_{ALFALFA} > 6.0$ [10]. Detections with $5.0 \lesssim \mathrm{SNR}_{ALFALFA} \lesssim 6.0$ typically were adjudicated as marginal.

3. Resulting large-scale structures

While we find galaxies over the entire observed redshift range, the majority lie within $2000 - 8000\,\mathrm{km\,s^{-1}}$. The velocity histogram (not shown here) shows a clear peak at $6000\,\mathrm{km\,s^{-1}}$, probably due to the prevalence of galaxies connected to the Perseus Pisces Super Cluster (PPScl) described below. There is a noticeable drop-off in detections upwards from $\sim 8000\,\mathrm{km\,s^{-1}}$ which is due to a combination of recurring RFI at $v > 8500\,\mathrm{km\,s^{-1}}$ and limited telescope sensitivity.

The new H I detections are distributed almost symmetrically about the Galactic equator, irrespective of Galactic latitude b (see the middle panel of Fig. 1, described below), confirming that the detection rate is independent of extinction and star density.

To investigate the large-scale structures revealed by these new detections we plot in Fig. 1 their spatial distribution in Galactic coordinates centred on the northern Milky Way. It includes 2MRS data up to latitudes of $|b| \geq 15^\circ$ to test for continuity of the newly identified features with previously known structures (filaments, walls, voids) at higher Galactic latitudes. The outlined rectangular region demarcates the NRT survey area.

The top panel shows the 2MRS galaxies with $K_s^o \leq 11\overset{\mathrm{m}}{.}25$, as well as data in the $|b| \lesssim 5^\circ$ strip from the Zcat ($K_s^o \leq 11\overset{\mathrm{m}}{.}25$) compilation by Huchra (priv comm). The middle panel displays the distribution of the 252 NIR-bright 2MASX galaxies detected with the NRT. In the bottom panel the new detections have been merged with the previously known data of objects to the $K_s^o \leq 11\overset{\mathrm{m}}{.}25$ completeness limit. In all three panels the galaxies are colour-coded by velocity: the $300 - 2500\,\mathrm{km\,s^{-1}}$ velocity range is shown in cyan, $2500 - 5000\,\mathrm{km\,s^{-1}}$ in blue, $5000 - 7500\,\mathrm{km\,s^{-1}}$ in black and the $7500 - 10000\,\mathrm{km\,s^{-1}}$ range in green. The black and blue colours coincide with the approximate velocity range of the PPScl.

When comparing the bottom and top panels (i.e., the status before and after the NRT observations) the power of revealing previously unknown large-scale structures in the ZoA through H I observations of intrinsically bright (extinction-corrected) NIR galaxies is quite obvious. Several prominent filaments and walls are now seen to cross the ZoA which were previously not – or at most marginally – visible. The most obvious filamentary structures cross the Galactic Plane at $\ell \approx 90^\circ$ (Cygnus), $\ell \approx 135^\circ$ (Cassiopeia), $\ell \approx 160^\circ$ (Perseus), $\ell \approx 180^\circ$, as well as the Puppis filament at $\ell \approx 240^\circ$ [11]. An underdense region of galaxies is apparent at $\ell \approx 120^\circ$ and $-2^\circ \lesssim b \lesssim 5^\circ$, stretching from $cz \approx 4000$ to $7000\,\mathrm{km\,s^{-1}}$. In the next sections we will discuss two of the most striking newly revealed features in more detail, namely the ones at $\ell \approx 90^\circ$ and $\ell \approx 160^\circ$.

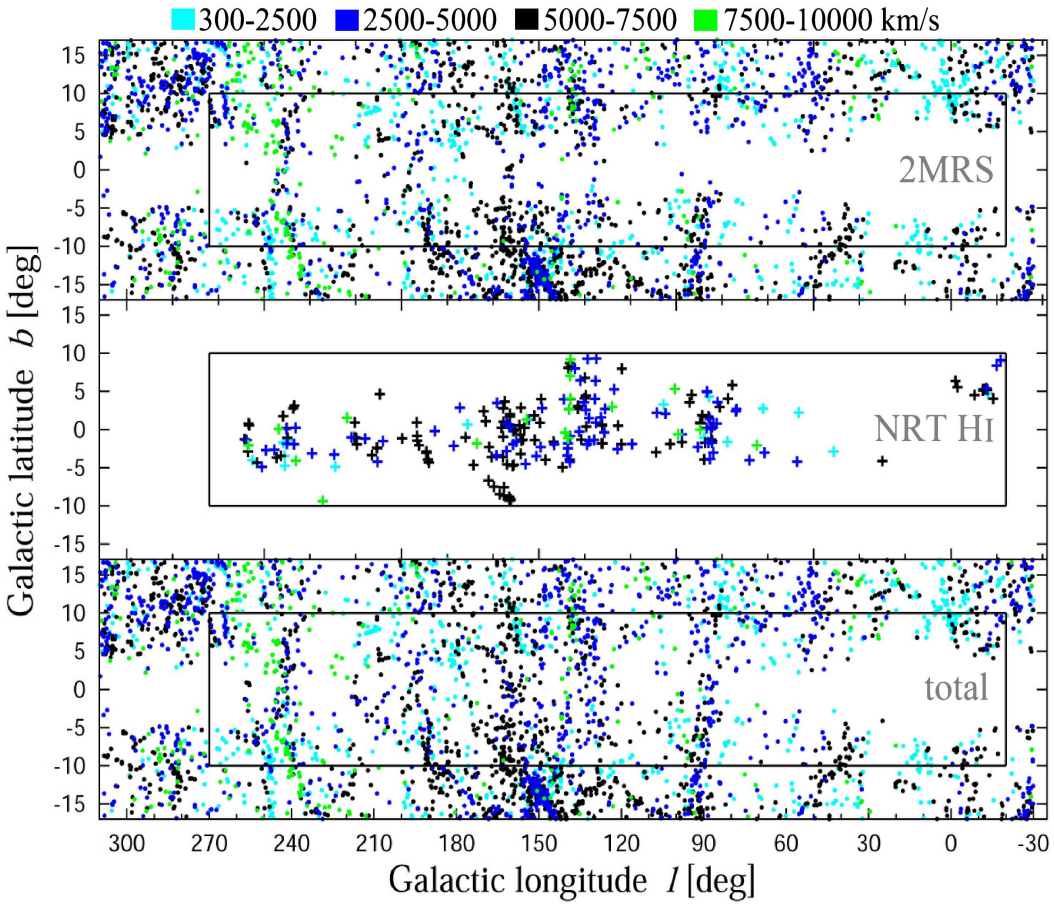

Figure 1. The spatial distribution of galaxies in Galactic coordinates in the ZoA. The survey area explored with the NRT is marked by the black rectangle. Galaxies are colour-coded by their velocity range, as shown at the top: the $300-2500\,\mathrm{km\,s^{-1}}$ velocity range is shown in cyan, $2500-5000\,\mathrm{km\,s^{-1}}$ in blue, $5000-7500\,\mathrm{km\,s^{-1}}$ in black and the $7500-10\,000\,\mathrm{km\,s^{-1}}$ range in green. The top panel shows the 2MRS galaxies ($K_s^o \leq 11\overset{\mathrm{m}}{.}25$) with known redshifts from Zcat (Huchra, priv comm) for low-latitude 2MASX galaxies. The middle panel displays the H I-detections obtained by us with the NRT. The bottom panel shows the combined data and emphasizes the links with previously known structures.

3.1. The Perseus extension of the second Perseus-Pisces arm

The first region of interest is seen in the constellation of Cygnus around $\ell \approx 90°$. It shows a very prominent filament that can be traced from below the Plane at $\ell, b \approx 90°, -10°$ extending up to the other side of the ZoA at a slight angle to $\ell, b \approx 100°, -10°$. This filament seems to form part of the second (eastern) Perseus-Pisces arm that emanates southwards from the Perseus A 426 cluster (ℓ,b) $\approx$ (150°,-13°), then bends backwards towards the Galactic plane (at about $\ell, b \approx 110°, -30°$; not shown here) and re-enters our plot at about $\ell, b \approx 80°, -15°$. Most previous studies of the PPScl assumed it to kind of stop and dissolve around $\ell, b \approx 90°, -10°$ as no signature was found of it in earlier optical galaxy searches [12], nor any indication of a continuation on the other side of the obscuring ZoA band. Our data clearly confirms such a continuation. It implies the eastern Perseus-Pisces chain to be considerably larger than evidenced in any previous survey of the PPScl complex.

3.2. A potentially massive cluster

The second prominent feature is a concentration of H I-detections at $\ell \approx 160^\circ$ right in the middle of the ZoA ($b = 0\overset{\circ}{.}5$). It lies within a nearly vertical (in Fig. 1) wall-like structure (at $v \approx 6000 \pm 1000\,\mathrm{km\,s^{-1}}$ in velocity space) and can be traced across the full width of the ZoA. It is interesting to note that within this wall, at the core of the galaxy concentration, we find two very strong radio galaxies. Their position and redshifts (6236 and 6655 km s^{-1} respectively; [13]) confirm that they reside inside the galaxy concentration. These are the head-tail radio source (3C 129) and the double-lobed giant elliptical radio galaxy (3C 129.1). The presence of such radio sources with bent lobe morphology usually is indicative of a rich cluster environment.

Focardi et al (1984) [14] were the first to put forward the idea of an extension of the Perseus-Pisces Complex across the ZoA towards the northern Galactic hemisphere that would link the Perseus cluster (A 426; $\ell, b, v \simeq 150^\circ, -13^\circ, 5000\,\mathrm{km\,s^{-1}}$) to Abell 569 ($\ell, b, v \simeq 168^\circ, 23^\circ, 5800\,\mathrm{km\,s^{-1}}$). It would traverse the Galactic Plane at the location of the two bright radio galaxies, which also coincides with the location where Weinberger (1980) ([15]) found an excess of galaxies in his early optical search (at $\ell \approx 160^\circ$). This connection has been much debated over the years (e.g., [16], [17], [18]), but no conclusive results were found due to the lack of (redshift) data in this dust-enshrouded region.

The suspicion that 3C 129 and 3C 129.1 form part of a massive cluster was later substantiated through the identification of the X-ray cluster CIZA J0450.0+4501 ([19]). The radio sources lie within the X-ray emission of the CIZA cluster and are at the same distance. With an X-ray luminosity of $L_\mathrm{X} = 1.89 \times 10^{44}\ \mathrm{h}_{50}^{-2}\mathrm{erg\ s^{-1}}$ this cluster is not among the brightest X-ray sources in ROSAT. For comparison, its flux is about 20% that of the Norma cluster A 3627, the central cluster of the Great Attractor [20] – which, as an aside, also hosts 2 radio sources, the central one a wide-angle tail source and the other also a head-tail source. With regards to the X-ray flux it should be noted, however, that the intervening high gas column density ($N_H \gtrsim 10^{21}\ \mathrm{cm^{-2}}$) in the Galaxy may well have reduced the flux of the low energy X-ray photons in the ROSAT $0.1 - 2.4\mathrm{keV}$ band, resulting in an underestimate of its luminosity. The cluster might therefore be more massive than its X-ray luminosity suggests. Despite its possible connection with the wider PPScl complex, it has not received much attention since.

4. Conclusions and future perspectives

The 252 H I detections in this previously unexplored northern region of the ZoA have revealed new and interesting structures that are clearly associated with the Perseus Pisces Super Cluster. These new structures seem to imply that the PPScl is more extended than previously thought and potentially much more massive, with the identified cluster in the $\ell \approx 160^\circ$ filament. This may well have implications for our understanding of the dynamics and flow-fields observed in this region.

To learn more about this cluster's role in, and its mass contribution to the PPScl, and its relation to the observed local flow fields, we therefore recently put in a proposal – and have been allocated time - to conduct a deep H I imaging survey over a $2\overset{\circ}{.}4 \times 2\overset{\circ}{.}4$ area (mosaiced) around this cluster with the Westerbork Synthesis Radio Telescope (WSRT).

Acknowledgements

This work is based upon research supported by the National Research Foundation and Department of Science and Technology. MR is grateful for the bursary provided by the South African SKA Project Office. This publication makes use of data products from the Two Micron All Sky Survey, which is a joint project of the University of Massachusetts and the Infrared Processing and Analysis Center, funded by the National Aeronautics and Space Administration and the National Science Foundation.

References

[1] Kraan-Korteweg R C 2005 *Reviews in Modern Astronomy* (*Reviews in Modern Astronomy* vol 18) ed S Röser pp 48–75

[2] Skrutskie M F, Cutri R M, Stiening R, Weinberg M D, Schneider S, Carpenter J M, Beichman C, Capps R, Chester T, Elias J, Huchra J, Liebert J, Lonsdale C, Monet D G, Price S, Seitzer P, Jarrett T, Kirkpatrick J D, Gizis J E, Howard E, Evans T, Fowler J, Fullmer L, Hurt R, Light R, Kopan E L, Marsh K A, McCallon H L, Tam R, Van Dyk S and Wheelock S 2006 *AJ* **131** 1163–1183

[3] Jarrett T H, Chester T, Cutri R, Schneider S E and Huchra J P 2003 *AJ* **125** 525–554

[4] Huchra J, Jarrett T, Skrutskie M, Cutri R, Schneider S, Macri L, Steining R, Mader J, Martimbeau N and George T 2005 *Nearby Large-Scale Structures and the Zone of Avoidance* (*ASP conf.* vol 329) ed A P Fairall & P A Woudt p 135

[5] Huchra J P, Macri L M, Masters K L, Jarrett T H, Berlind P, Calkins M, Crook A C, Cutri R, Erdoğdu P, Falco E, George T, Hutcheson C M, Lahav O, Mader J, Mink J D, Martimbeau N, Schneider S, Skrutskie M, Tokarz S and Westover M 2012 *ApJS* **199** 26

[6] Kraan-Korteweg R C and Lahav O 2000 A&A Rev. **10** 211–261

[7] Masters K L, Springob C M and Huchra J P 2008 *AJ* **135** 1738–1748

[8] Henning P A, Springob C M, Minchin R F, Momjian E, Catinella B, McIntyre T, Day F, Muller E, Koribalski B, Rosenberg J L, Schneider S, Staveley-Smith L and van Driel W 2010 *AJ* **139** 2130–2147

[9] Donley J L, Staveley-Smith L, Kraan-Korteweg R C, Islas-Islas J M, Schröder A, Henning P A, Koribalski B, Mader S and Stewart I 2005 *AJ* **129** 220–238

[10] Saintonge A 2007 *AJ* **133** 2087–2096

[11] Kraan-Korteweg R C and Huchtmeier W K 1992 A&A **266** 150–166

[12] Seeberger R, Huchtmeier W K and Weinberger R 1994 A&A **286** 17–24

[13] Spinrad H 1975 *ApJL* **199** L1

[14] Focardi P, Marano B and Vettolani G 1984 A&A **136** 178–180

[15] Weinberger R 1980 A&AS **40** 123–127

[16] Chamaraux P, Cayatte V, Balkowski C and Fontanelli P 1990 A&A **229** 340–350

[17] Lu N Y and Freudling W 1995 *ApJ* **449** 527

[18] Pantoja C A, Altschuler D R, Giovanardi C and Giovanelli R 1997 *AJ* **113** 905–936

[19] Ebeling H, Edge A C, Bohringer H, Allen S W, Crawford C S, Fabian A C, Voges W and Huchra J P 1998 *MNRAS* **301** 881–914

[20] Kraan-Korteweg R C, Woudt P A, Cayatte V, Fairall A P, Balkowski C and Henning P A 1996 *Nature* **379** 519–521